Preprints of the 18th IFAC World Congress
Milano (Italy) August 28 - September 2, 2011

Upper Limb Flexion Assistance Based on Minimum-Jerk Trajectory Using Wearable Motion-Assist Robot

Takeshi Enya * **Michi Yamane** * **Hiroyuki Nakamura** **
Takaaki Aoki *** **Yutaka Nishimoto** **** **Ken'ichi Yano** †

* *Faculty of Engineering, Department of Human and Information Systems, Gifu University, 1-1 Yanagido, Gifu 501-1193, Japan*
** *Faculty of Engineering, Department of Mechanical Engineering, Mie University, 1577 Kurimamachiya-cho, Tsu City 514-8507, Japan (e-mail:nakamura@robot.mach.mie-u.ac.jp)*
*** *Department of Rehabilitation and Orthopedics, Gifu University Hospital,1-1 Yanagido, Gifu City 501-1194, Japan (e-mail: ujimiya@gifu-u.ac.jp)*
**** *Department of Surgical Nursing, Gifu University School of Medicine, 1-1 Yanagido, Gifu City 501-1194, Japan (e-mail: yutaka@gifu-u.ac.jp)*
† *Faculty of Engineering, Department of Mechanical Engineering, Mie University, 1577 Kurimamachiya-cho, Tsu City 514-8507, Japan (e-mail:yanolab@robot.mach.mie-u.ac.jp)*

Abstract: In this paper, we propose a robotic system to assist patients who have upper limb dysfunction in performing reaching movements through flexion. Since upper-limb motion is more strongly needed than lower limb mobility for near work, a patient's level of recovery of upper-limb function influences daily life. Recently, with the widespread application of robotic technology in rehabilitation medicine, it is often noted that moving actively is more important than moving passively to enable rapid recovery. Human reaching movement is known to conform to the standard minimum-jerk, which is characterized by a bell-shaped velocity waveform with a single peak. Patients with dysfunction move their extremities if they are capable of controlling the motor movement of their upper limb, but are assisted by the robot when they cannot do so. The range of movement is estimated from the motor control based on minimum-jerk criterion.

We currently carry out research and development of various assistive robots for upper limb movements including power assist robots to supplement the shortage of medical practitioners and caregivers (Tsukahara et al. [2009]). If a robot can instead assist the patient, home rehabilitation is possible. Robots support those with dysfunction of the upper limb which leads to rehabilitation, improved quality of life, and reduced burden on medical practitioners and caregivers. Many rehabilitation robots have been developed, but they are implemented with a joystick to compensate for reduced limb function. In addition, there are a few master-slave robots, but these have shortcomings that limit practicality and independence of patients. Also, many power assist robots assist patients on the basis of pressure sensor data obtained from the physical operating forces. Most robots, however, utilize systems that are input amplifier based and cannot be used by people who do not have the range of motion (ROM) to exert sufficient force. Therefore, we developed an assistive robot for upper limb movement that has high rehabilitation effectiveness. By using a robot in daily life, patients can recover from dysfunction. Our robot enables flexion and extension of the elbow by providing reaching movement support that takes into account the expanding range of motion of a joint. This reaching movement support method is based on estimating the trajectory of the participant's reaching movement.

⋆ This work was supported by Regional Innovation Cluster Program (City Area Type): Southern Gifu, Japan Area.

1. ASSISTIVE ROBOT FOR UPPER LIMB MOVEMENT

The assistive robot for upper limb movement developed in this study is shown in Fig. 1, and its link structure is shown in Fig. 2. This robot has a manipulator with 4 degrees of freedom, and supports flexion and extension of the elbow. The drive axis is only in the first joint of the robot, while the second joint is a free joint for medial and external elbow rotation. The third joint is a prismatic joint with the flexibility to meet individual forearm-length. The forth joint is a free joint and is used for pronation and supination of the wrist. These free joints contribute to the free motion of the upper limb. Our motion assist robot is equipped with a DC motor that has a maximum torque and speed of 4.2[Nm] and 226[deg/s], respectively. These values are based on the results of a preliminary experiment examining elbow joint torque and operation speed (elbow joint torque: 4[Nm], operation speed: 150[deg/s]). The

exterior of the robot and upper limb guard are made of acrylonitrile butadienestyrene resin (ABS resin) to reduce the robot's weight. A super-thin film pressure sensor detects the force applied by the user. Four sensors are installed on the robot and measure the forces of flexion and extension, as well as medial and external rotation of the elbow by determining the fixed pressure between the robot and the human arm. The robot is attached to the upper limb by a shoulder supporter (see Table 1 for the robot's specifications).

Fig. 1. Upper limb motion assist robot

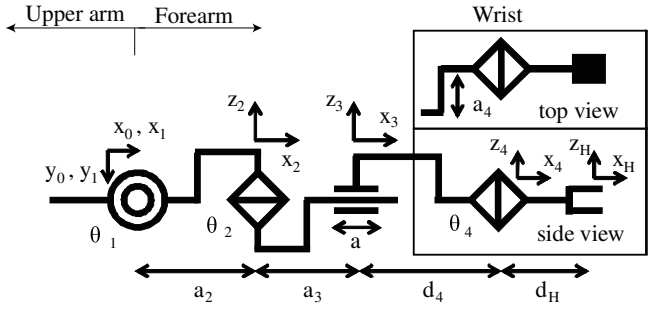

Fig. 2. Structure of upper limb motion assist robot

Table 1. Specifications of the upper limb support robot

Weight of robot	0.9[kg]
Range of movement	120[deg]
Gear ratio of motor	159
Max. speed of motor	6000[rpm]
Max. torque of motor	44[mNm]
Encoder resolution	512[p/rev]

2. HUMAN MODELING

A human joint is driven by at least two skeletal muscles, and one muscle often drives two joints. Therefore, it is difficult to design a human musculoskeletal model, but recently this area has come to be actively researched. Among the many models, the model proposed by Ito et al. is straightforward.

In their model, the power of muscle F is expressed by Eq. (1):

$$F = u - kux - bu\dot{x}. \tag{1}$$

Here, u, k, and b are the contraction force, elasticity, and viscosity of the muscle, respectively; x is the amount of muscle contraction; and q is the angle of rotation. Each muscle undergoing flexion and extension exert torque T_f and T_e, respectively, as expressed in Eq. (2) and Eq. (3) on the condition that both flexion and extension muscles have equivalent mechanical impedance:

$$T_f = d(u_f - ku_f q - bu_f \dot{q}), \tag{2}$$

$$T_e = d(u_e - ku_e q - bu_e \dot{q}). \tag{3}$$

The torque driving the elbow, τ_h, is expressed as the difference between muscle flexion and muscle extension:

$$\tau_h = d\{(u_f - u_e) - (u_f + u_e)(kq + b\dot{q})\}. \tag{4}$$

The motion equation of the elbow that considers muscle is expressed by Eq. (5), where M_h is inertia and g_h is gravity:

$$M_h\ddot{q} + g_h(q) = d\{(u_f - u_e) - (u_f + u_e)(kq - b\dot{q})\}. \tag{5}$$

Next, the robot is modeled. In general, we express the motion equation of a multijoint manipulator as

$$M_r\ddot{q} + C_r\dot{q} + g_r(q) = \tau_r, \tag{6}$$

where M_r, C_r, and g_r are coefficients describing the inertia, viscosity, and gravity of the robot, respectively, and τ_r is driving torque of the robot. This robot is a manipulator with 4 degrees of freedom, but the drive axis has only one joint. Therefore, we can approximate the robot by using the single-degree-of-freedom (SDF) motion equation expressed by Eq. (7):

$$M_r\ddot{q} + g_r(q) = \tau_r. \tag{7}$$

Assuming that the robot and human are coordinated, the motion equation for the entire system is expressed as Eq. (8):

$$\begin{aligned}(M_r + M_h)\ddot{q} + g_r(q) + g_h(q) &= \tau_r + \tau_h,\\ M\ddot{q} + g(q) &= \tau.\end{aligned} \tag{8}$$

System control is expressed as Eq. (9) where the power amplifier gain is k.

$$\tau_r = k\tau_h \tag{9}$$

3. MOTION ASSIST WITH VARIABLE DAMPING METHOD

In general, mechanical impedance in near work results from high inertia and low viscosity. On the other hand, inertia is low and viscosity is high during a rapid movement (Ikeura [2006]). In this study, position-based variable damping control was applied to the robot. Viscosity changes depended on the control force (Takesue et al. [2007]), while variable damping was based on the force applied by the operator and had a unique feature in line with the bell-shaped velocity curve, which is well known

to reflect the ideal trajectory of the reaching movement of the human arm (Uno et al. [1989]). The control law is given by Eq. (10) and Eq. (11):

$$k_{amp}\tau_h = M_I\ddot{\theta}_d + D_I\dot{\theta}_d, \tag{10}$$

$$D_I = D_s \cdot \frac{1}{\frac{|\tau_h|}{A} + 1}, \tag{11}$$

where M_I and D_I are the inertia and viscosity for mechanical impedance, respectively, D_s and A are the initial viscosity and the reduction rate of viscosity of variable damping, respectively, and τ_h and k_{amp} are the human's control force and the amplifier's rate of force, respectively. Additionally, for the sake of safety improvements, the a rate inhibition coefficient is added for the target trajectory. The weighting factor W conforms to the following condition and is expressed as Eq. (12).

- $\dot{\theta}_d > 0$ and $\frac{ROM}{2} < \theta_d \leq ROM$
- $\dot{\theta}_d < 0$ and $0 \leq \theta_d < \frac{ROM}{2}$

$$W = -\frac{4}{ROM^2}\theta_d^2 + \frac{4}{ROM}\theta_d \tag{12}$$

The results of the variable damping control are shown in Fig. 3. Input τ_h is the positive value of the sinusoidal wave (amplitude 1.0[Nm], frequency π[rad/s]), and the other parameters are $M_I = 2.0 \times 10^{-4}$[Nm/(deg/s^2)], $\tau_k = 0$[Nm], $A = 0.05$[-], and $D_s = 0.05$[Nm/(deg/s)]. This control method represents the natural trajectory of joint motion because the velocity waveform is bell-shaped.

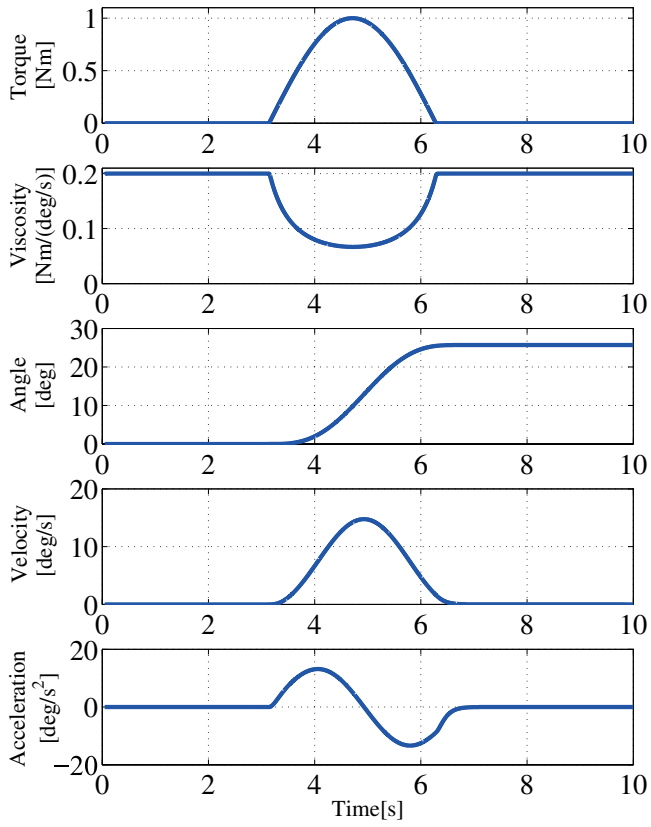

Fig. 3. Experimental result of control-force-based variable damping

4. TRAJECTORY ESTIMATE

4.1 reaching movement

Reaching movements that extend the arm to the target seem to be simple operations as they are performed without giving conscious thought to the action. However, the brain plans the trajectory subconsciously. Because trajectory of the hand is in straight line at any time and because the velocity waveform is bell-shaped (horizontal axis shows time) in a wide-range reaching movement, it is possible to express the evaluation function, as demonstrated by Flash and Hogan, where the jerk is assumed to be minimum:

The trajectory can be obtained analytically by minimizing the solution of the evaluation function (Flash et al. [1985]). The cost function of the jerk is expressed by Eq. (13) and the trajectory is given by Eq. (14) and (15).

$$E_J = \int_0^{T_f} \left(\frac{d^3x}{dt^3}\right)^2 + \left(\frac{d^3y}{dt^3}\right)^2 dt, \tag{13}$$

$$x(t) = x_0 + (x_f - x_0)\left(6s^5 - 15s^4 + 10s^3\right), \tag{14}$$

$$y(t) = y_0 + (y_f - y_0)\left(6s^5 - 15s^4 + 10s^3\right) \tag{15}$$

where T_f is total movement time and s is the normalized value of physical time t divided by T_f. $(x_0,\ y_0)$ are the coordinates of the origin, and $(x_f,\ y_f)$ are coordinates of the terminal.

4.2 estimated trajectory

Variable damping control as explained above cannot help people with limited range of joint motion because this method is the same as the conventional power-assist method. In the case of assisting people with dysfunction of the upper limb, the amplification of force must be very large. Although it is possible that this method could assist such people, the system could become unpredictable and dangerous.
To solve this problem, we have adopted predictive control, which estimates reaching position when the user cannot initiate movement through application of sufficient force. This control is based on the actual motion within the range of the user's intended motion. In other words, the control system estimates the intended movement during the estimating interval as shown in Fig. 4.

The reaching motion consists of acceleration and deceleration intervals. There are three estimated motions as shown in Fig. 5

(1) For acceleration, deceleration occurs after additional acceleration
(2) For deceleration, deceleration continues
(3) For constant velocity, velocity is maintained

If the estimated motion is that of Case 1 or Case 2, the estimated trajectory of velocity can be approximated as the minimum-jerk trajectory. The estimated trajectory is defined by Eq. (19) based on the sampled velocity data $(v_0,\ v_1,\ v_2)$ with the sampling interval T in the estimating interval:

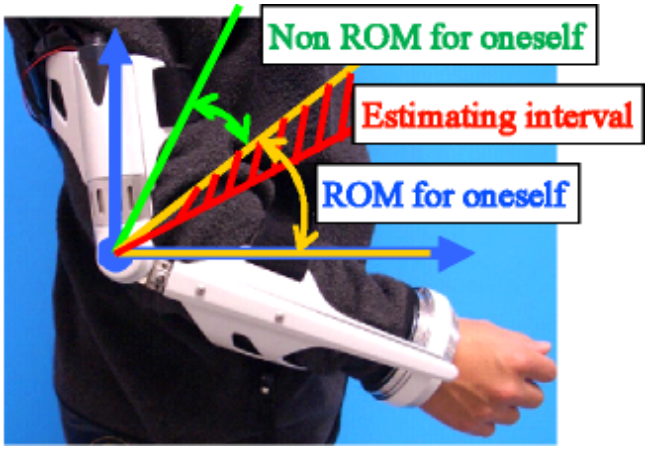

Fig. 4. Definition of joint range of motion

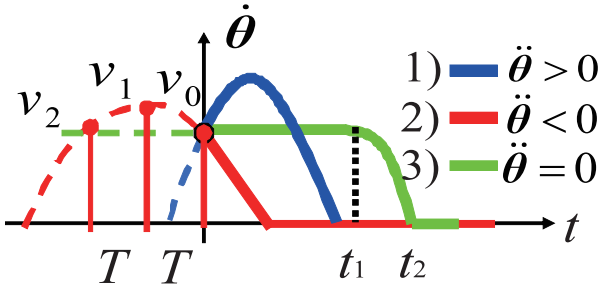

Fig. 5. Estimated trajectory of reaching movement

$$\dot{\theta}_{est} = \frac{30R}{T_f^5}\{(t+T_x)(t+T_x-T_f)\}^2, \tag{16}$$

$$T_x = \frac{T}{\gamma}(-\alpha \pm \sqrt{\alpha^2 - \beta\gamma}), \tag{17}$$

$$T_f = \frac{\sqrt{v_1}T_x^2 - \sqrt{v_0}(T_x - T)^2}{\sqrt{v_1}T_x - \sqrt{v_0}(T_x - T}, \tag{18}$$

$$R = \frac{v_0 T_f^5}{30T_x^2(T_x - T_f)^2}. \tag{19}$$

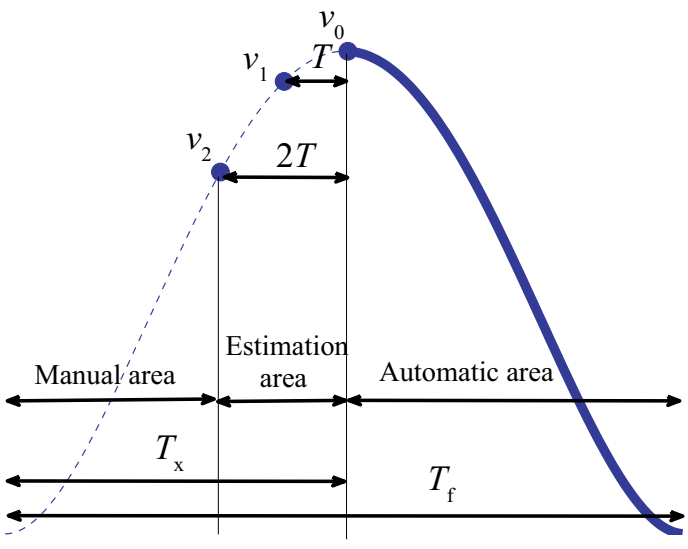

Fig. 6. Parameters and areas of operating modes

As shown in Fig. 6, T_x is the time when automatic changes occur in the predicted orbit. The horizontal axis represents time and the vertical axis represents velocity. R is angle displacement $\theta_f - \theta_0$.

$$\alpha = 4v_1 - \sqrt{v_1 v_2} - 3\sqrt{v_0 v_1} \tag{20}$$

$$\beta = 8\sqrt{v_0 v_1} \tag{21}$$

$$\gamma = 2\sqrt{v_1 v_2} + 2\sqrt{v_0 v_1} - 4v_1 \tag{22}$$

The trajectory based on the velocity can be approximated by Eq. (19), if the robot accelerates or decelerates during the estimating interval. However, if the robot transitions from acceleration to deceleration, the trajectory cannot be approximated from the velocity. In this case, the robot uses the result of Eq. (23). If the result of Eq. (23) is negative, it is assumed that $H = -1$ and then the sampling interval will be changed from T to ϵT, and recalculated. $(0 < \epsilon < 1)$

$$S = \sqrt{v_1 v_2} + \sqrt{v_0 v_1} - 2v_1 \tag{23}$$

$$H = \begin{cases} 1 & for\ S > 0 \\ -1 & for\ S \le 0 \end{cases} \tag{24}$$

For $T_x - \epsilon T$ and $T_x - 2\epsilon T$, the velocity data sampled are v_{11} and v_{21}, respectively. In experiments, we focused on the velocities v_0, v_{11}, v_1 and sampling interval $\epsilon = \frac{1}{2}$. The calculations results show that when the change in velocity is too large, movement time T_f is prolonged, and velocity of the robot rapidly becomes zero. Zero velocity is at the halfway point of the estimated trajectory when the robot reaches its ROM limit. To overcome the problem, we adopted the following equations, in which a new trajectory of velocity can be calculated, where, θ_{xf} is the angle of displacement from T_x to T_f, θ_{max} is the maximum flexion angle, θ_a is the invariable angle at maximum flexion, θ_{max} is the angle of the movable range, and θ_c is the invariable angle at which the user cannot initiate movement.

$$\theta_a = \theta_{max} - \theta_c \tag{25}$$

The maximum velocity based on the minimum-jerk trajectory is expressed by Eq. (26):

$$v_{max} = 1.875\frac{R_2}{T_{f2}}, \tag{26}$$

where R_2 is the displacement angle. The velocity at the switching angle is assumed to be at maximum velocity. R_2 and T_{x2} are described as follows

$$R_2 = 2\theta_a \tag{27}$$

$$T_{x2} = \frac{1}{2}T_{f2} \tag{28}$$

Therefore, the velocity after reaching the switching angle is expressed by Eq. (29):

$$\dot{\theta}_{est2} = \frac{30R_2}{T_{f2}^5}\{(t+T_{x2})(t+T_{x2}-T_{f2})\}^2. \tag{29}$$

In contrast, if the estimated motion reflects Case 3, it can be assumed that maintaining the same velocity is desired, but the timing of deceleration cannot be estimated. In this case, the estimated trajectory is defined by Eq. (30) and Eq. (31) identifies this motion as deceleration after

maintaining the velocity for a certain period of time. v_1 is the velocity when switching to automatic control, t_1 is the duration of uniform motion, and t_2 is the termination time of motion; t_1 and t_2 are determined through a trial and error process.

$$if\ t < t_1 \quad \dot{\theta}_{est} = v_1 \tag{30}$$

$$if\ t \geq t_1 \quad \dot{\theta}_{est} = -\frac{v_1}{t^2}(t - t_1)^2 + v_1. \tag{31}$$

4.3 switching input

The system switches into automatic mode when the switching angle is detected, and switches into manual mode when velocity becomes zero. There is no discontinuity when switching into automatic mode. However, there is discontinuity when switching into manual mode, as the robot must lift the upper limb because the participant cannot exert the necessary muscle force to accomplish this movement without assistance. It is dangerous to switch into manual mode from auto mode when the sensor is still measuring an applied force. An offset of the first-order lag element avoids this phenomenon and is shown in Fig. 7. The robot follows the trajectory obtained from the variable damping control and the estimated reaching trajectory control according to PID control. The total control system is shown in Fig. 8. The PID parameters are proportional gain $K_P = 0.5$, integral gain $K_I = 0.1$, and differential gain $K_D = 0.01$.

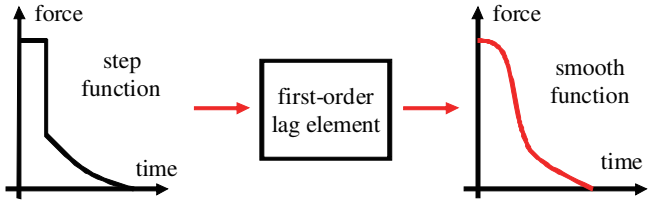

Fig. 7. Smoothing discontinuous trajectory according to the first-order lag element

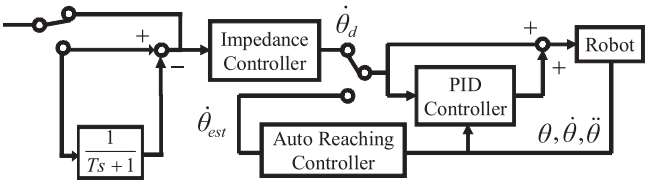

Fig. 8. Motion assist control based on trajectory estimation of reaching movement

5. EXPERIMENT

The result of using the discriminant function H is shown in Fig. 9. In Fig. 9, the first graph shows input to the variable damping control, the second graph shows determination of the control mode, the third graph shows discriminant function H, the fourth graph shows the angle, the fifth graph shows the velocity, and the sixth graph shows the estimated velocity. The blacked-out area is controlled in automatic mode. Parameters of variable damping are $M = 0.0002$ [Nm/(deg/s^2)], $D_0 = 0.05$[Nm/(deg/s)], $A = 0.05$[-] and the switching angle is 25[deg]. By virtue of the discriminant function H, the robot can respond to changes in velocity (acceleration or deceleration) in the estimating interval. The result of estimation accuracy is shown in Fig.

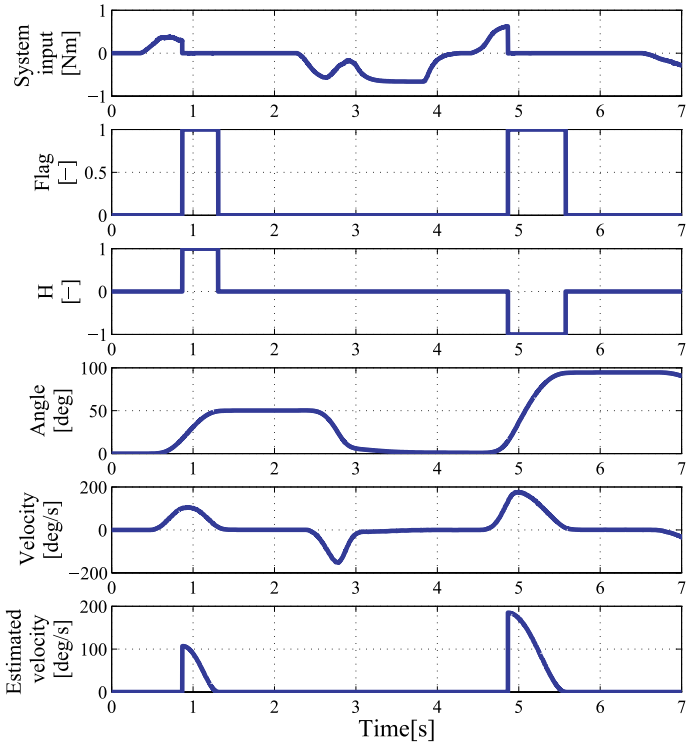

Fig. 9. Experimental result of discriminant function

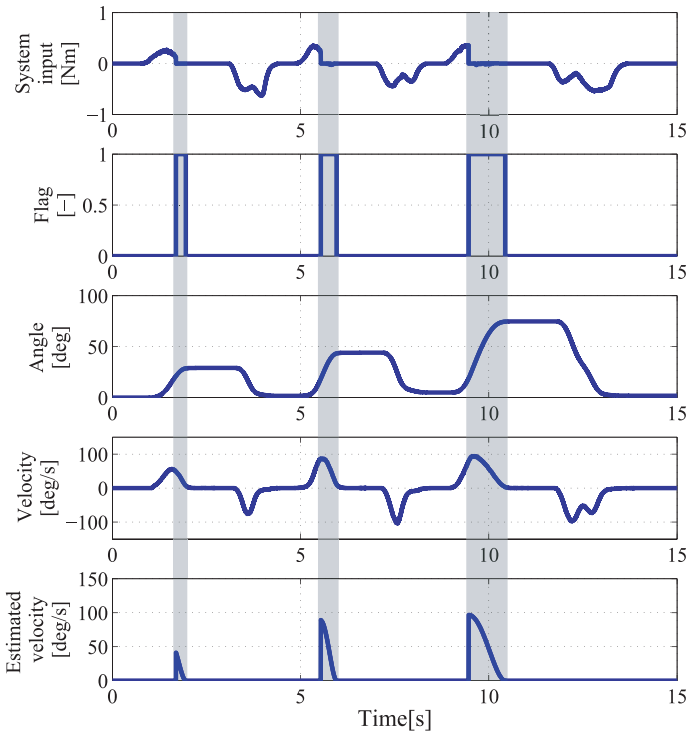

Fig. 10. Experimental result of reaching angle estimation

10. In this experiment, the user flexes the elbow at each target angles of 30, 50, and 80[deg]. The parameters are the same as those in the previous experiment. Although the ±5[deg] error exists, this experiment produced an excellent result because the system did not demand positioning

accuracy. The velocity waveform was bell-shaped, and the system was controlled continuously and smoothly even when the reaching position was distant. For the case where the predicted displacement exceeds the maximum angle, the estimated result of using $\dot{\theta}_{est2}$ is shown in Fig. 11. In Fig. 11, the first graph shows input to the variable damping control, the 2nd graph shows determination of the control mode, the third graph shows angle, the fourth graph shows velocity, and the fifth graph shows estimated velocity. The dotted line shows the trajectory before recalculation that is rapidly approaching 0. In contrast, after recalculation, the velocity form is bell-shaped.

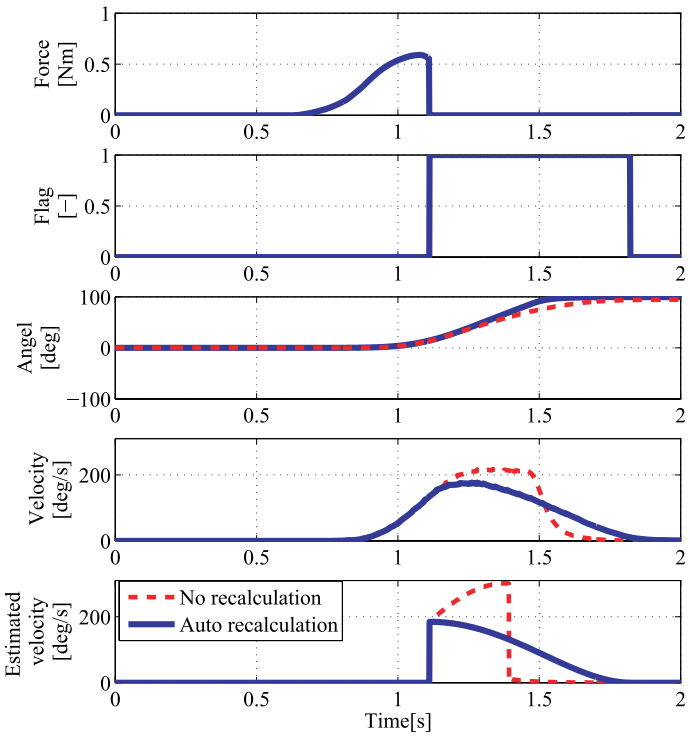

Fig. 11. Experimental result of auto recalculation

This system was tested by a patient with a brachial plexus injury. In this type of injury, the brachial plexus is damaged by excessive impact and is typical of motorcycle accidents. The participant could flex the elbow to 40[deg] but not over 40[deg] by using muscle force. The participant was only assisted by variable damping control and by variable damping control with the reaching motion-assist method. The result is shown in Fig. 12. The maximum extension angle of the participant was set to 0[deg], the range of joint motion achieved by the participant's own muscle force was 0 $\sim$ 30[deg], the estimated range was 25 $\sim$ 30[deg], while the range of joint motion achieved by robotic assistance was 30 $\sim$ 100[deg]. With variable damping only, the participant could not flex their elbow above 40[deg], even if flexion was rapid and intense. But, with variable damping of the reaching motion-assist method, the participant could flex the elbow to 50[deg] in the first motion and then to 85[deg] in the second motion. As shown by the results, this system can estimate the arbitrary reaching angle, and in doing so is efficacious.

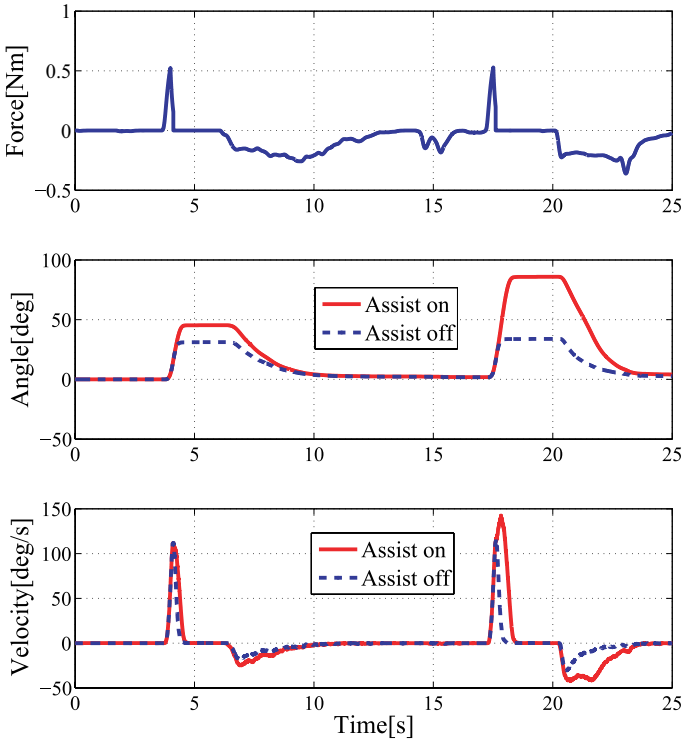

Fig. 12. Experimental result using participant's data

6. CONCLUSIONS

Here, we proposed a motion-assist method based on the minimum-jerk trajectory estimation of the reaching motion. The effectiveness of this method was revealed in a clinical setting by kinesthetic sense data of a patient with a brachial plexus injury. Results revealed that this system provides effective reaching motion assistance to people who cannot achieve a desired range of joint motion on their own.

REFERENCES

T. Flash, N. Hogan. The coordination of arm movement : An experimentally confirmed mathematical model *Journal of Neuroscience*, 5 1688–703, 1985.

R. Ikeura Control of Assist Devices Based on physical Characteristics of Human Being. *Journal of the Society of Instrument and Control Engineers*, 45, 5 413–418, 2006.

N. Takesue, R. Kikuuwe, A. Sano, H. Mochiyama, H. Sawada and H. Fujimoto Force-Dependent Variable Damping Control for Positioning Task Assist. *Journal of the Robotics Society of Japan*, 25, 2 306–313, 2007.

A. Tsukahara, Y. Hasegawa and Y. Sanaki Standing-Up Motion Support for Paraplegic Patient with Robot Suit HAL *Proc. IEEE Intl. Conf. Rehabilitation Robotics* 211–217, 2009.

Y. Uno, M. Kawato and R. Suzuki Formation and control of optimal trajectory in human multijoint arm movement. *Biological Cybernetics*, 61, 2 89–101, 1989.